

## A vibration control strategy using variable stiffness joints

Qinyu Wang <sup>\*a</sup>, Gennaro Senatore <sup>b</sup>, Vasiliki Kaymenaki<sup>c</sup>, Arjan Habraken<sup>a</sup>, Patrick Teuffel<sup>a</sup>

<sup>a</sup> Chair of Innovative Structural Design (ISD), TU/e 5600MB Eindhoven NL, \*Q.wang2@tue.nl

<sup>b</sup> Applied Computing and Mechanics Laboratory (IMAC, ENAC); Swiss Federal Institute of Technology (EPFL)

<sup>c</sup> Department of Civil Engineering, TU Delft

### Abstract

Adaptive joints are structural joints made of materials with enhanced transduction properties that can vary their stiffness via solid-state actuation (e.g. thermal, mechanical). In this work, stiffness tuning is used to switch the joint between a ‘locked’ (e.g. a moment connection) and a ‘released’ (e.g. pin) state. Previous work has looked into the feasibility of using variable stiffness joints during shape and force control in order to reduce actuation work. This paper focuses on control of the structure dynamic response to loading. The natural frequency of the structure is tuned to escape dangerous resonance conditions in two ways: 1) a geometric reconfiguration via large shape changes or 2) via the change of stiffness of the joints. Two case studies are considered: 1) an active frame integrated with four actuators fitted on tubular elements which are connected by a shape memory polymer joint 2) a planar truss structure. Experimental tests on the active frame have shown that by varying the length of the linear actuators, large shape changes can be employed to effectively change the natural frequency of the structure. During shape change, the joint stiffness is lowered to ease geometric reconfiguration. For the planar truss case study, simulations have shown that the ‘release’ or ‘locking’ of multiple joints can be employed to change the eigenfrequencies, the more so the higher the eigenmode.

**Keywords:** Variable stiffness joints, adaptive structures, shape control, natural frequency tuning, vibration control

### 1. Introduction

Adaptive structural joints can vary their stiffness via solid-state actuation because they are made of materials with enhanced transduction properties. Amongst commercially available products, shape memory polymers (SMPs) feature large stiffness variations from a glassy state to a rubbery state during phase transition. SMPs are cross-linked. Crosslinks are the connections between polymer segments that form the three-dimensional network-like structure at molecular level [1]. Crosslinks form or break depending on whether the material is above or below the transition temperature causing a drastic increase or reduction respectively of the elastic modulus as shown experimentally by Tobushi et al [2] and Liu et al [3]. SMP phase transition is activated under an external stimulus. A review of SMPs activation methods is given in Leng et al. [1], Meng & Jinlian [4]. Suitable stimuli including temperature, light, electric and magnetic fields can trigger a drastic change from a temporary shape to an original shape the material has been trained to “remember”.

SMPs have found application in aerospace engineering for shape control of aircraft wings (Barbarino et al [5], Liu et al [6], Keihl et al [7]) but also in smart textiles [1] as well as in deployable structures [1]. Fibre reinforced SMP has been tested in a deployable hinge used in a solar array prototype by Lan et al [8]. A SMP composite with embedded shape memory alloy (SMA) [9] has been used in a wind-responsive façade systems by Lignarolo et al [10]. The façade comprises components made of SMA strips embedded in a SMP matrix. The façade components change shape to control ventilation for indoor climate optimization. Experimental work by Markopoulou [11] has tested SMP for shape control of a small-scale frame structure arranged in triangular modules based on an origami pattern. The SMP joints are laser-cut and placed at the intersection between adjacent modules. A heat source triggers the phase change in the joints which soften thus allowing the structure to be easily deformed via external actuation.

Variable stiffness capabilities have been employed for vibration control of structures to improve safety and serviceability during strong loads (i.e. strong winds, earthquakes) or harmful resonance (Du et al [12], Ledezma-Ramirez et al [13, 14], Philip et al [15] and Soong et al [16, 17]). Filipe et al [18] investigated the use of SMA springs as linear actuators to control shape changes of a tensegrity tower to tune the dynamic response of the structure. Previous work by Senatore et al [19] investigated the use of variable stiffness joints for shape and force control in order to reduce actuation work and increase control accuracy. Experimental tests have shown that stiffness variation to support with quasi-static loads is feasible.

This work focuses on the use of variable stiffness joints to change the dynamic response of structures under loading. Two strategies are investigated: (1) a geometric reconfiguration via large shape changes and (2) change of stiffness of the structural joints. This paper is organized in three main sections presenting: 1) material testing of the SMP polymer employed for experimental testing; 2) experimental testing of an active frame integrated with four actuators fitted on tubular elements connected by a shape memory polymer joint; 3) simulation studies on a 2D truss structure whose joints can be ‘locked’ or ‘released’ to change behaviour from moment transferring to pin connection.

## 2. SMP material properties

This first section aims at characterizing the behaviour of the material employed in experimental testing discussed in section 3 as well as for the simulations studies in section 4.

The structural joints proposed in this study are made of polyurethane-based shape memory polymer (SMP) MM 5520 [20]. SMP belongs to a class of materials that are able to change their stiffness reversibly under the influence of an external stimulus such as temperature. To characterize the thermomechanical behaviour of this material, a Dynamic Mechanical Analysis (DMA) has been carried out using a DMA Q800 analyser [21] on a SMP prismatic sample of dimensions 10mm x 2mm x 0.17mm. An oscillatory strain produced by a deformation of 10  $\mu\text{m}$  along the main axis of the sample is applied with a frequency of 1Hz. During the test, the sample is placed in a temperature chamber. The temperature is increased from 40°C to 90°C with a heating rate of 1°C/min. DMA measures the complex modulus of the material which is made of two parts 1) the storage modulus and 2) the loss modulus. The storage modulus is what is usually referred as Young’s modulus  $E$  of the material, whereas the loss modulus represents the lost energy due to friction between the molecular chains and heat. Figure 1(a) shows the storage modulus ( $E'$ ) as a function of the temperature.

Upon heating, the SMP specimen undergoes through three different states: glassy, transition and rubbery. The storage modulus decreases as the temperature increases resulting in a loss of stiffness and subsequently in large deformations. When the specimen reaches the threshold temperature, the material changes phase and a significant reduction of the elastic modulus occurs. Although the specimen has been fabricated via additive manufacturing, the transition temperature from glassy to rubbery phase is approximately 63°C which is in the range reported in [22]. That being said, it has been observed that the angle of the infill pattern can influence the transition temperature and the stiffness and thus further investigation is needed.

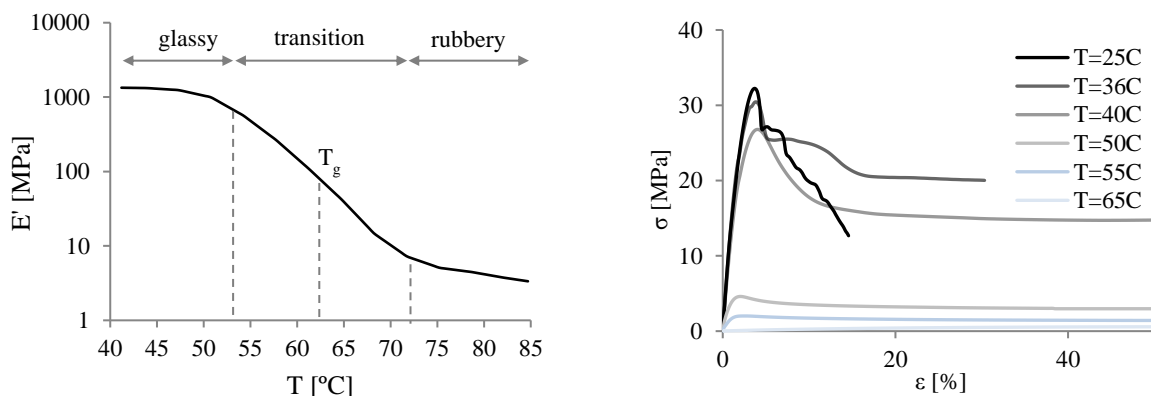


Figure 1: (a) storage modulus vs temperature, (b) stress vs strain curve at various temperatures

Tensile tests have been carried out to characterize the ultimate strength using the same equipment employed for the dynamic mechanical analysis described before. The DMA Q800 can apply a maximum force of 10N, the specimen can be strained up to 150%. Stress variation as a function of the strain is reported in Figure 1(b). Table 1 gives the tensile strength and elongation at yield under different temperature condition. At low temperatures, the sample breaks at a low strain thus behaving as a brittle material. Upon heating, the behavior changes from brittle to ductile – a substantial drop in the stress due to necking is recorded. Beyond the glass transition temperature, the mechanical behavior of the SMP becomes rubbery as the strain can reach values up to several hundred percent before failure. Experimental tests indicate that after the transition phase SMP material strength reduces drastically and hence it might not be able to withstand significant loads. The use of reinforcement is thus necessary if used as a structural bearing material.

Table 1: Tensile strength and strain at yield

Temperature [°C]	$\sigma$ [MPa]	$\epsilon$ [%]
25	32.23	3.72
36	30.44	3.82
40	26.80	4.00
50	4.60	2.00
55	2.01	1.90
65	0.63	0.15

Along with experimental tests, SMP material behaviour has been simulated using a software called ANSYS workbench 18.1. Figure 2 (a) and (b) show the storage modulus ( $E'$ ) and the damping factor ( $\tan\delta$ ) respectively as a function of the temperature. The damping factor is a measure of the energy dissipated as the temperature increases representing mechanical damping or internal friction in a viscoelastic system. Note that the damping factor increases substantially during the transition phase and remains two orders of magnitude higher when the material is the rubbery state compared to when it is in a glassy state. This suggests that there is potential for application in vibration control of structures. Since there is a good agreement between numerical and experimental results, material simulation based on viscoelastic theory [23] will be employed in future work to analyse more complex structural layouts.

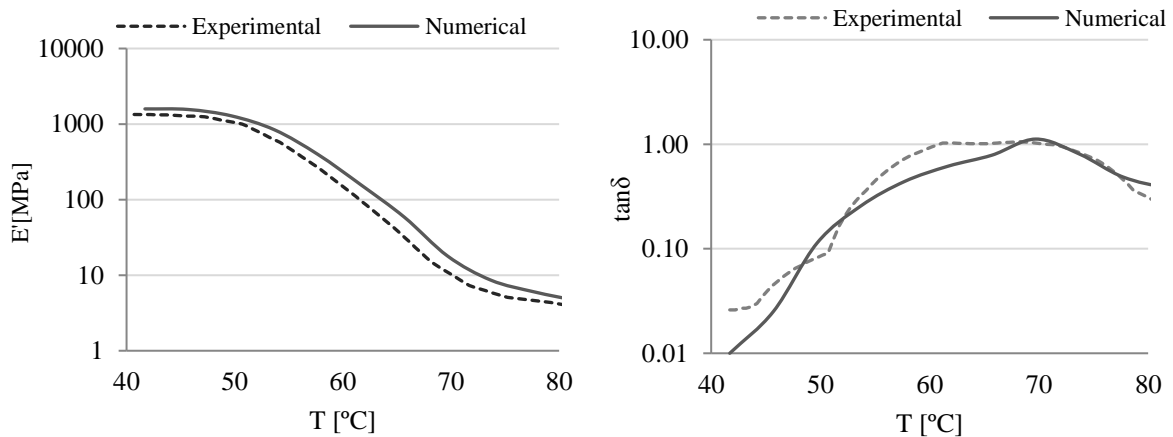


Figure 2: (a) storage modulus and (b) damping factor as a function of the temperature

### 3. Experimental Testing

#### 3.1 4-element active frame

The structure under testing is an active frame made of four elements connected by a variable stiffness joint. The main dimensions and type of support of the frame are shown in Figure 3. The elements are aluminium tubular sections whose outside diameter is 20mm with a wall thickness of 2mm. Each

element of the frame is integrated with an electric linear actuator. The stroke of each actuator is 300 mm. The linear actuators (PC32 model with AKM33E motor) are manufactured by Thomson Linear.

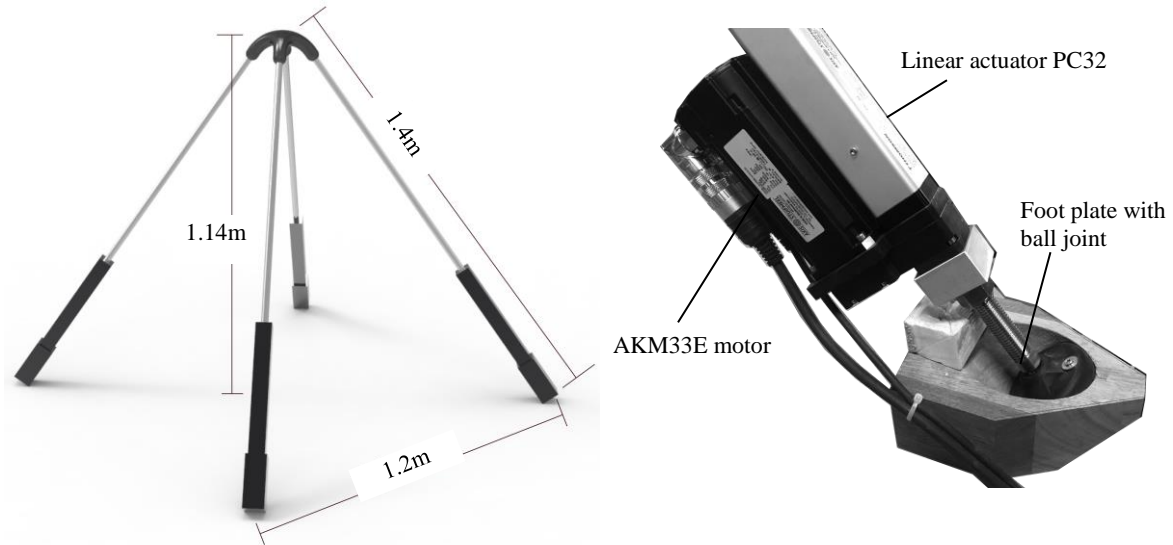


Figure 3: (a) 4-element frame dimensions, (b) foot plate with ball joint

The joint is made of the same SMP polymer discussed in section 2 and it has been fabricated via fused deposition modelling. Resistive heating is used as activation method. A pattern made of 2-mm diameter through holes was drilled to allow a 1-mm diameter nickel-chromium heating wire to pass through. As discussed in the conclusion of section 2, at the 'rubbery' state the material is not able to withstand structural loads. In the 'released' state the joint should work between a moment connection and a pin allowing relative motion of the elements it connects to. To avoid excessive elongations, Kevlar shape memory polymer composite (SMPC) skin is applied in layers arranged in several directions to cover the surface of the joint as shown in Figure 4. The elastic modulus of the skin is 1.3 GPA along the direction of the fibres.

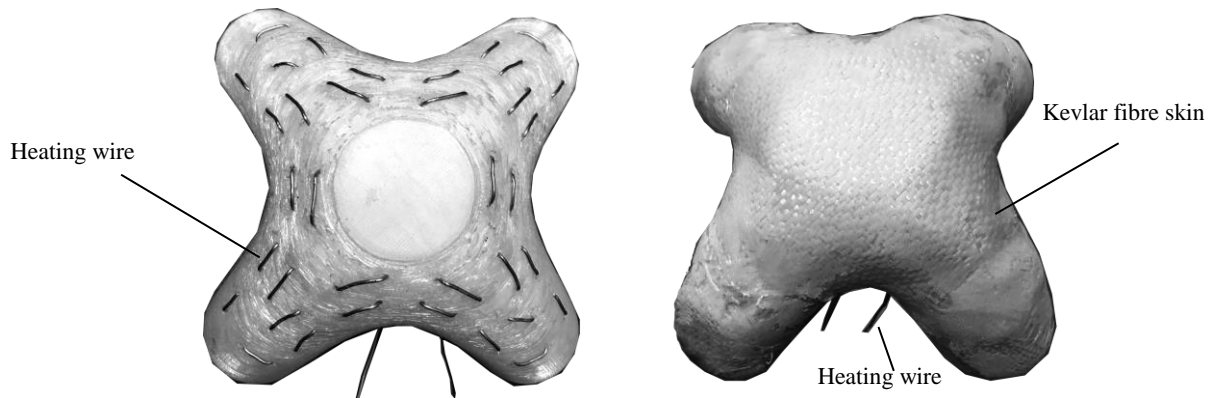


Figure 4: (a) heating wire pattern, (b) Kevlar fibre reinforcement

### 3.2 Eigenfrequency shift via change of shape and joint stiffness

The aim of this experimental study is to appreciate to what extent the fundamental frequency of the 4-element frame described in the previous section can be controlled via a shape change as well as joint stiffness variation. An accelerometer (AP37) is fitted to the SMP joint as indicated in Figure 5. The structure is excited by an impulse force applied on the opposite side the accelerometer is fitted onto.

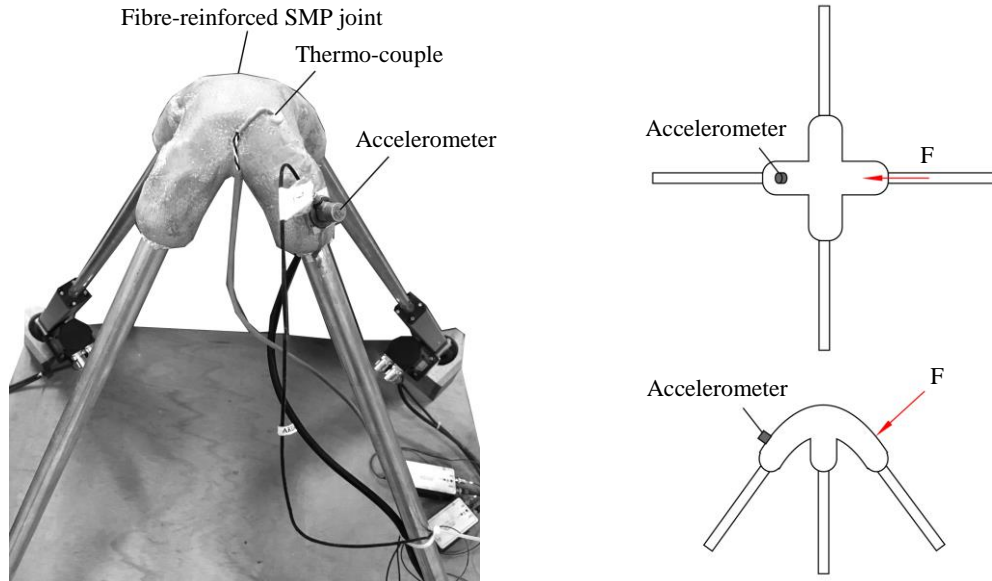


Figure 5: accelerometer location

For brevity, the shape changes will be indicated using the actuator length change vector ( $\Delta L1, \Delta L2, \Delta L3, \Delta L4$ ). The actuator length changes are expressed in dm. For example, when none of the actuators changes length, the shape is indicated as (0,0,0,0) and when all actuators are at maximum stroke (300 mm) the shape change is indicated as (3,3,3,3). Four shape changes are performed (0, 0, 0, 0) (1, 1, 1, 1) (2, 2, 2, 2) and (3, 3, 3, 3). Measurements are taken after a shape change is completed before and after the joint stiffness is varied. Each measurement is taken 10 times. Recorded accelerations are averaged out to reduce noise. The measurement is processed to obtain the power spectral density which is plotted in Figure 6.

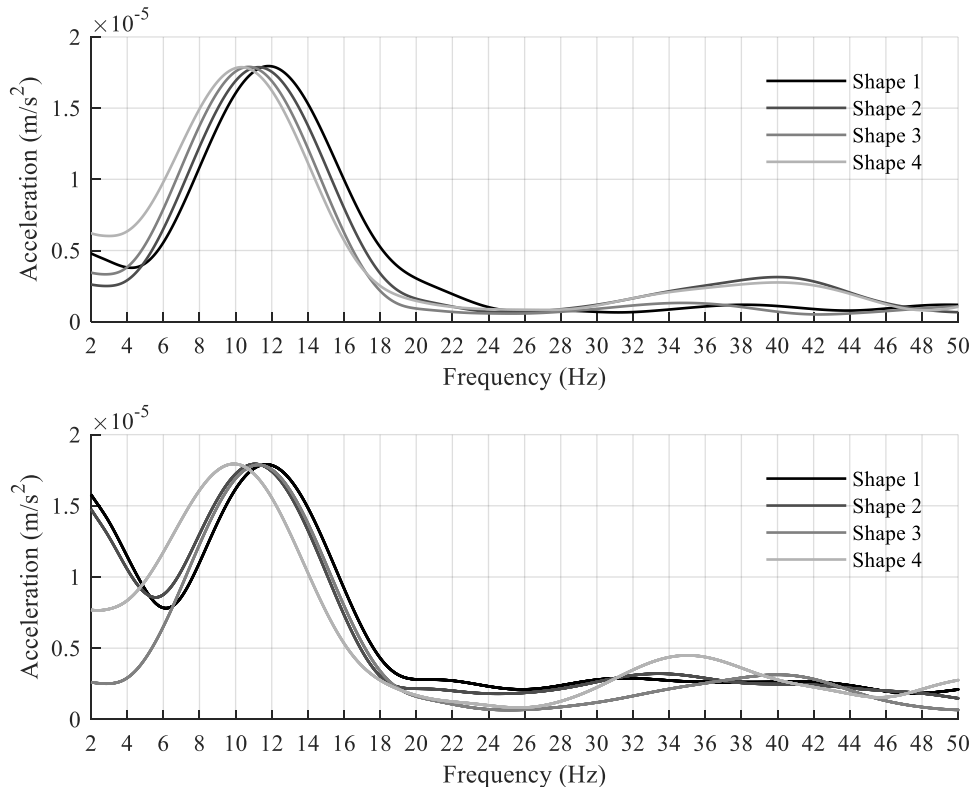


Figure 6: Acceleration vs. Frequency (a) joint before and (b) after heating

The fundamental frequency decreases as the height of the structure increases moving from Shape 1 (0,0,0,0) to Shape 4 (3,3,3,3). When the joint is not actuated, the fundamental frequency reduces from 11.82 Hz (Shape 1) to 10.32 Hz (Shape 4) which is a shift of 12.69%. When the joint stiffness is actuated, the fundamental frequency reduces further to 9.90 Hz (Shape 4) which is a shift of 16.23%.

## 4. Simulation studies

### 4-element frame

The frequency shift of the 4-element frame has been simulated using a software called Oasis Gsa. The elements are modelled as ‘beams’ whose length is changed to simulate shape changes. The mass matrix of the structure is computed using the element shape functions (consistent mass matrix). The element end rotational degrees of freedom are released to simulate the change of stiffness of the node. It was found that the simulated frequency shift is in good accordance with the experimental one when the stiffness of the released degrees of freedom is set to 27 Nm. In this case when no degree of freedom is released, the fundamental frequency shifts from 11.90 Hz (Shape 1) to 10.58 Hz (Shape 4). When the element degrees of freedom are released, the fundamental frequency shifts further to 9.94 Hz.

### 4.1. Simply supported truss

The structure considered in this case is a statically indeterminate planar truss whose span and height are 10 m and 2 m respectively as indicated in Figure 7. The truss is simply supported. The elements are circular hollow section made of steel (S235). The element outside diameter is 50 mm with a 5 mm wall thickness.

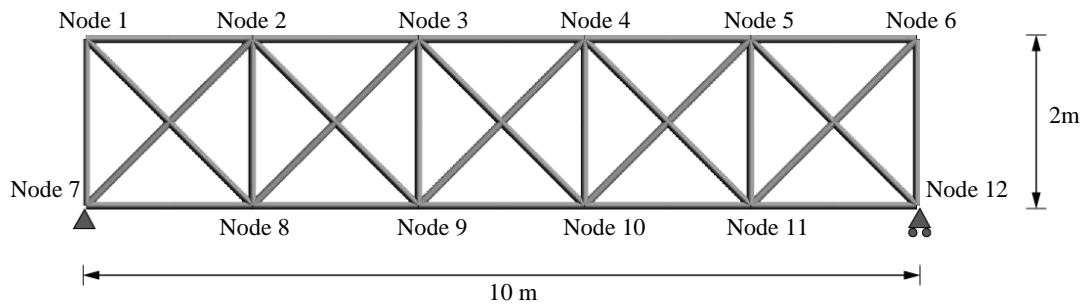


Figure 7: simply supported planar truss

Table 2: fundamental frequencies of first modes

# of released nodes	Mode 1	Mode 2	Mode 3	Mode 4	Mode 5
0	8.712	14.88	27.95	32.04	32.91
1	8.711	14.87	21.17	27.95	32.03
2	8.71	14.85	20.87	21.4	27.97
3	8.709	14.61	15.33	20.93	27.54
4	8.707	13.98	15.13	16.39	24.1
5	8.706	13.95	15.13	16.3	20.84
6	8.705	13.91	15.12	16.22	20.74
7	8.703	13.66	14.93	15.24	16.96
8	8.701	13.48	14.47	15.17	15.91
9	8.701	13.47	14.45	15.17	15.88
10	8.701	13.46	14.43	15.16	15.85
11	8.701	13.45	14.37	15.16	15.74
12	8.7	13.43	14.31	15.15	15.64

Simulations have been carried out to appreciate the frequency shift as the nodes change from fixed to released. The truss is assumed to be part of a roof or bridge supporting system. Each bay of the truss supports a  $10 \text{ m}^2$  subsidiary area out of plane. A dead load of  $3 \text{ k N/m}^2$  is assumed to be applied on the top chord. The dead load is converted to mass for the modal analysis. The mass matrix is computed using the element shape functions (consistent mass matrix).

Change of stiffness of a node is simulated by releasing the rotational degrees of freedom of the elements that connect to it. Table 2 gives the values of the first five natural frequency changes as the nodes are released progressively from one to all nodes. The values are averaged over node release combinations. Frequency shift in percentage terms are 0.14%, 9.74%, 48.80%, 52.72% and 52.48% for the first 5 modes. The change of eigenfrequency as a function of the number of released nodes is shown in Figure 8.

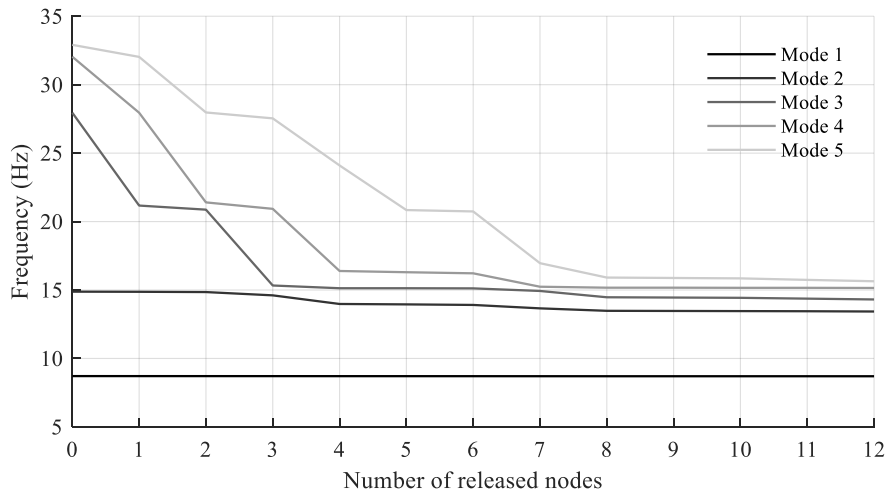


Figure 8: frequency shift as a function of the number of released nodes

## 5. Conclusion

This paper discusses simulation and experimental studies to investigate the feasibility of controlling the structure dynamic response via stiffness tuning. Controlled shape change and joint stiffness change are employed as a means to tune the eigenfrequency of the structure. The joint of the structure is made of a shape memory polymer (SMP) reinforced with Kevlar. Testing showed that this SMP based composite can be modelled as a viscoelastic material with good accuracy.

Experimental tests of a 4-element active frame have shown that shape change is more effective to tune the eigenfrequency of the structure compared to the effect of node stiffness variation. This has been confirmed by simulations of a planar truss. Node stiffness variation has been simulated by releasing the element (beam) end rotational degrees of freedom. Through node stiffness change there is a little variation of the eigenfrequency for low eigenmodes which are of interest for civil engineering applications.

Further work involves studies that define the generality of this conclusion by investigating the efficacy of controlling the dynamic response of the structure through a combination of shape change and node stiffness change. In addition, future work will look into quantifying the increase in damping that occurs when the joint stiffness is reduced. Although node stiffness change on its own might not be generally effective to tune the frequency of low eigenmodes, the increase in damping might be employed to reduce the dynamic response during resonance.

## Acknowledgements

The authors would like to thank 4TU.Bouw Lighthouse Project Programme 2017, China Scholarship Council (CSC) and EPFL Applied Computing and Mechanics Laboratory (IMAC) for supporting this work.



## References

- [1] J. Leng, X. Lan, Y. Liu and S. Du, "Shape-memory polymers and their composites: Stimulus methods and applications," *Progress in Materials Science*, vol. 56, no. 7, p. 1077–1135, 2011.
- [2] H. Tobushi, H. Hara, E. Yamada and S. Hayashi, "Thermomechanical properties in a thin film of shape memory polymer of polyurethane series," *Smart Materials and Structures*, vol. 5, no. 4, p. 483, 1996.
- [3] Y. Liu, K. Gall, M. L. Dunn, A. R. Greenberg and J. Diani, "Thermomechanics of shape memory polymers: Uniaxial experiments and constitutive modeling," *International Journal of Plasticity*, vol. 22, no. 2, p. 279–313, 2006.
- [4] Q. Meng and H. Jinlian, "A review of shape memory polymer composites and blends," *Composites: Part A*, vol. 40, p. 1661–1672, 2009.
- [5] S. Barbarino, E. I. Saavedra Flores, R. M. Ajaj, L. Dayyani and M. I. Friswell, "A review on shape memory alloys with applications to morphing aircraft," *Smart Materials and Structures*, vol. 23, no. 6, 2014.
- [6] Y. Liu, H. Du, L. Liu and J. Leng, "Shape memory polymers and their composites in aerospace applications: a review," *Progress in Materials Science*, vol. 56, no. 7, pp. 1077–1135, 2011.
- [7] M. M. Keihl, R. S. Bortolin, B. Sanders, S. Joshi and Z. Tidwell, "Mechanical Properties of Shape Memory Polymers for Morphing Aircraft Applications," *International Society for Optics and Photonics*, vol. 5762, pp. 143–152, 2005.
- [8] X. Lan, Y. Liu, H. Lv, X. Wang, J. Leng and S. Du, "Fiber reinforced shape-memory polymer composite and its application in a deployable hinge," *Smart Materials and Structures*, vol. 18, no. 2, p. 024002, 2009.
- [9] L. C.M.J.L, K. Jansen and P. Teuffel, "Mechanical characterization of a shape morphing smart composite with embedded shape memory alloys in a shape memory polymer matrix," *Journal of Intelligent Material Systems and Structures*, vol. 27, no. 15, pp. 2038–2048, 2016.
- [10] L. Lignarolo, C. Lelieveld and P. Teuffel, "Shape morphing wind-responsive facade systems realized with smart materials," in *Proceedings of the International Adaptive Architecture Conference*, 2011.
- [11] A. Markopoulou, "Design Behaviors; Programming Matter for Adaptive Architecture," *Next Generation Building*, vol. 2, no. 1, pp. 57–78, 2015.
- [12] D. Haiping, L. Weihua and N. Zhang, "Semi-active variable stiffness vibration control of vehicle seat suspension using an MR elastomer isolator," *Smart materials and structures*, vol. 20, no. 10, p. 105003, 2011.
- [13] D. Ledezma-Ramirez, N. Ferguson and M. Brennan, "Shock isolation using an isolator with switchable stiffness," *Journal of Sound and Vibration*, vol. 330, no. 5, p. 868–882, 2011.
- [14] D. Ledezma-Ramirez, N. Ferguson and M. Brennan, "An experimental switchable stiffness device for shock isolation," *Journal of Sound and Vibration*, vol. 331, no. 23, p. 4987–5001, 2012.
- [15] P. Bonello, M. J. Brennan and S. J. Elliott, "Vibration control using an adaptive tuned vibration absorber with a variable curvature stiffness element," *Smart Materials and Structures*, vol. 14, no. 5, p. 1055, 2005.
- [16] T. T. Soong, "State of the art review: active structural control in civil engineering," *Engineering Structures*, vol. 10, pp. 74–84, 1988.
- [17] T. Soong and J. Chang, "Active vibration control of large flexible structures," *Shock Vib. Bull.*, vol. 52, pp. 47–54, 1982.
- [18] F. A. dos Santos, A. Rodrigues and A. Micheletti, "Design and experimental testing of an adaptive shape-morphing tensegrity structure, with frequency self-tuning capabilities, using shape-memory alloys," *Smart Materials and Structures*, vol. 24, no. 10, p. 105008, 2015.
- [19] Q. Wang, S. Gennaro, H. Bier and P. Teuffel, "The Use of Variable Stiffness Joints in Adaptive Structures," in *International Association for Shells and Spatial Structures 2017*, Hamburg, 2017.
- [20] S. Technologies, "SMP Technologies," 2009. [Online]. Available: <http://www2.smptechno.com/en/smp/>. [Accessed 25 04 2018].
- [21] DMA, "TA instruments," [Online]. Available: <http://www.tainstruments.com/q800/?lang=de>. [Accessed 30 04 2018].
- [22] H. Tobushi, R. Matsui, K. Takeda and E. Pieczyska, *Mechanical Properties of Shape Memory Materials*, New York: Nova Science Publishers, 2013.
- [23] J. Diani, Y. Liu and K. Gall, "Finite Strain 3D Thermoviscoelastic Constitutive Model for Shape Memory Polymers," *Polymer Engineering and Science*, vol. 46, no. 4, pp. 486–492, 2006.